
Dimmable LED Lighting with a High-Efficiency DC-DC Converter with Twin Bus

Ch. Usha Sri¹, Rajesh Thota², B.Nagaraju³, Mysa Aparna⁴, K.Srinivasan⁵

^{1, 2, 3, 4} Assistant Professor, Department of Electrical and Electronics Engineering, Vaagdevi College of Engineering, Warangal, Telangana-506005, India.

⁵ Associate Professor, Department of Electrical and Electronics Engineering, Vaagdevi College of Engineering, Warangal, Telangana-506005, India.

Abstract—An improved twin-bus converter with $n + 1$ active switches is presented to enable dimming of n -string LEDs from true zero to the rated current level. This design offers greatly reduced voltage stresses, allowing the current-loop regulation switches to operate at very high frequencies while maintaining high efficiency across a wide load range. The dimming switch, on the other hand, operates at a lower frequency to ensure efficiency and prevent light flicker. The paper describes the detailed power stage working concept and individual string current control technique for the presented converter. Experimental results from a 3-string 50-W LED driver hardware prototype demonstrate that the independent string current for dimming control can be adjusted from zero to the required 350 mA. With a switching frequency of 1.08 MHz, a peak efficiency of 98.3% was achieved.

Index Terms—Dimmable LED drive, asymmetric multiple-level converter, high efficiency, light-emitting diode (LED), off-line LED illumination, three-level converter, two-input buck.

1. INTRODUCTION

White LEDs are rapidly becoming a preferred solid-state light source due to their high efficacy, extended lifetime, low environmental impact, and smooth dimming capabilities. One of the primary applications for LEDs is off-line lighting, such as general illumination, LCD backlights for desktop displays and televisions, and street and parking lot lighting, where multiple strings of LED driving techniques are often required.

There are four types of LED driving systems for dimming control: 1) analogue dimming with linear regulators; 2) PWM dimming with linear regulators; 3) pulse width modulation (PWM) dimming with linear regulators; and 4) PWM dimming with switching regulators. In analogue dimming methods, the LED current level of each string is adjusted by altering the reference level of the individual current feedback loop. This approach is quick and inexpensive but can result in color variation.

To achieve brightness adjustment without color variation over the full dimming range, PWM dimming methods have been introduced. In these methods, the amplitude of the pulsating LED current is kept constant, and the pulse width is regulated. Both linear and switching regulators can be used in either analog or PWM dimming methods. The efficiency of LED drivers with switching regulators is higher than that of drivers with linear regulators. Therefore, the PWM dimming method with switching regulators is the trend for future LED driving systems due to its high efficiency and better illumination quality. This paper discusses a further enhanced PWM dimming method with switching regulators aimed at off-line LED lighting applications.

In prior work, a two-input buck post-regulator was introduced to effectively reduce voltage stress across semiconductors while achieving high efficiency through parallel power processing [11] [12]. However, this approach is not suitable for PWM dimmable LED applications due to the limited output voltage range between the two input voltages [12]. This limitation results in the inability to dim the LED current to zero [16]. Although the configuration presented in [16] suggests inserting two active switches and one diode during the off-state of PWM dimming to block the two input voltages and achieve zero output voltage, this approach leads to higher conduction losses and increased system complexity, thereby hindering efficiency improvement.

To address these challenges, this letter proposes an improved two-input buck converter with $(n + 1)$ active switches for dimming n -string LEDs from true zero to the desired current level. By significantly reducing voltage stressors, the n -switches responsible for current-loop regulation can achieve high efficiency at very high frequencies, similar to the two-input buck converter. Additionally, the addition of one more dimming switch, controlled at a low frequency and shared by the n -string LEDs, ensures high-efficiency operation and full-range dimming from zero. The unique twin-bus-based LED driver is introduced to enhance efficiency, reduce inductor size, and expand the dimming range of the LED current simultaneously. Section II will provide a detailed explanation of the power stage working concept and control scheme of the proposed converter.

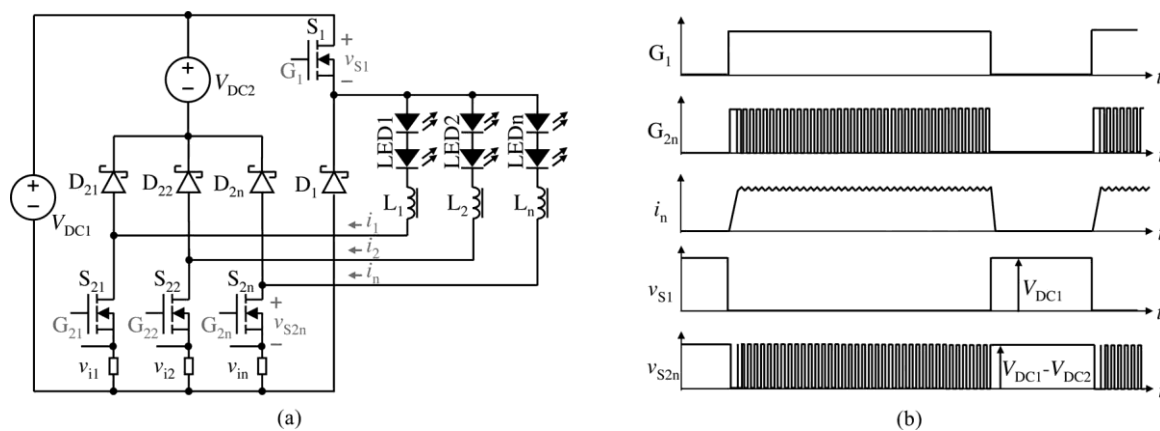


Fig. 2 illustrates the proposed converter, showcasing its circuit diagram and key waveforms.

To validate the circuit's operation and claimed performance, a 50-W high-brightness LED lighting hardware prototype was constructed and tested in various applications.

The operational principles of the novel converter are essential for understanding its functionality. The circuit architecture and key waveforms are depicted in Figs. 2(a) and (b), respectively. These include two input voltage sources, V_{DC1} and V_{DC2} , $(n + 1)$ power MOSFETs denoted as S_1 and S_{2n} , freewheeling diodes represented by D_1 and $D_{21} - D_{2n}$, and n output inductors labeled as $L_1 - L_n$. Notably, the AC-DC converter regulates the initial input voltage V_{DC1} slightly above the maximum voltage of the LED strings. A second input voltage, V_{DC2} , slightly lower than the minimum voltage of the LED strings at the specified current, is obtained using an appropriate turns ratio. Both input voltage sources, being close and shared, are referred to as the twin bus.

By adjusting the pulse width of the dimming switch S_1 , which operates at a low frequency of 400 Hz in this scenario, the average current of all LED strings can be controlled. Moreover, the voltage stresses of all S_{2k} and D_{2k} (where $k = 1, 2, \dots, n$) are simply the difference between the two input voltages, which are much lower than the input voltage and the desired output voltage level. This characteristic allows for the utilization of lower on-resistance MOSFETs and Shockley diodes with lower forward voltage drop. Additionally, the resistors in series with the low-side switches, which share the common ground, serve as cost-effective current sensors for the LED strings.

The proposed circuit combines features of two alternative converter topologies: the standard buck and the floating buck with twin bus. It is a three-level converter for dimmable LED driving, offering various duty cycles and switching frequencies between the high- and low-side active switches. This structure operates in four distinct modes during a single PWM dimming cycle, as depicted in Fig. 3. Specifically, the dimming switch S_1 remains ON when the LEDs are turned on, as illustrated in Fig. 3(a).

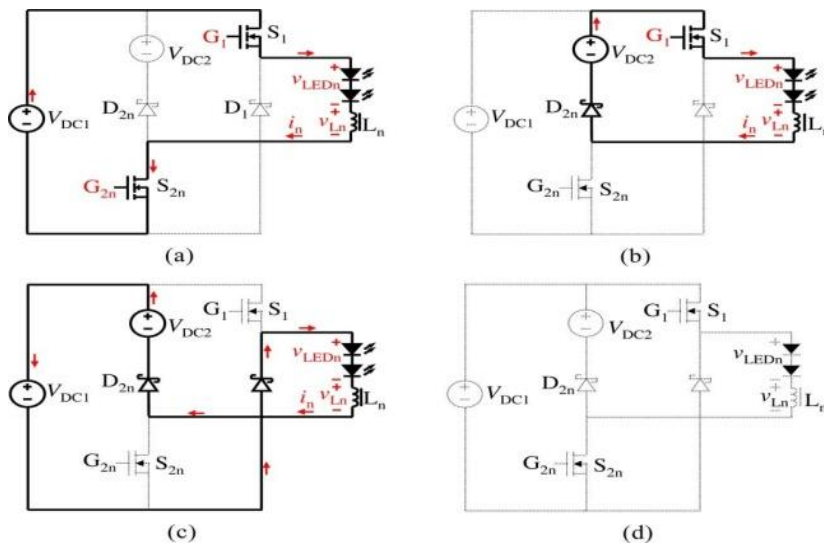


Fig. 3 illustrates the topological modes of the proposed converter, depicting four distinct intervals: (a) charging interval, (b) discharging interval, (c) resetting interval, and (d) idle interval of the output inductor.

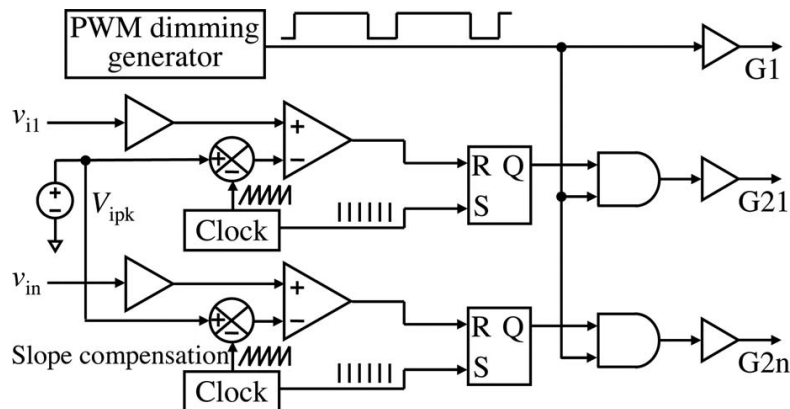


Fig. 4 illustrates the controller block diagram of the proposed converter.

The voltage stresses of the bottom switch S2n and its freewheeling diode D2n can be calculated using the formula:

$$V_{\max} = V_{DC1} - V_{DC2}$$

This equation (1) indicates that voltage stresses can be significantly reduced if VDC2 is configured to be near VDC1, resulting in reduced conduction losses.

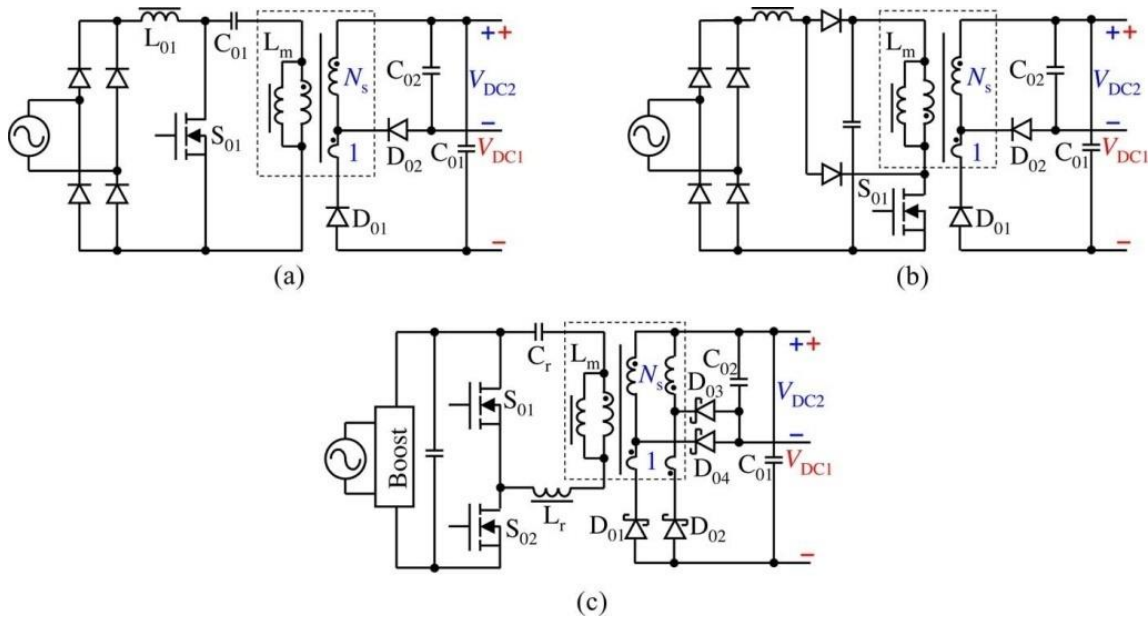


Fig.5. illustrates the twin-bus implemented circuits, showcasing three different configurations: (a) SEPIC, (b) single-switch boost-flyback converter, and (c) boost cascaded with LLC resonant converter.

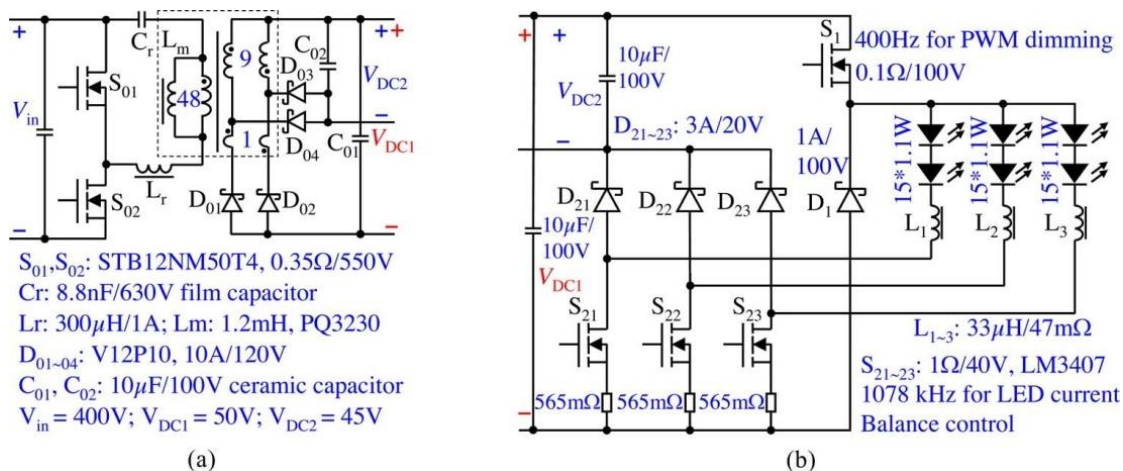


Fig.6. displays the power circuit and the parameters of the prototype: (a) LLC resonant converter, and (b) twin-bus converter.

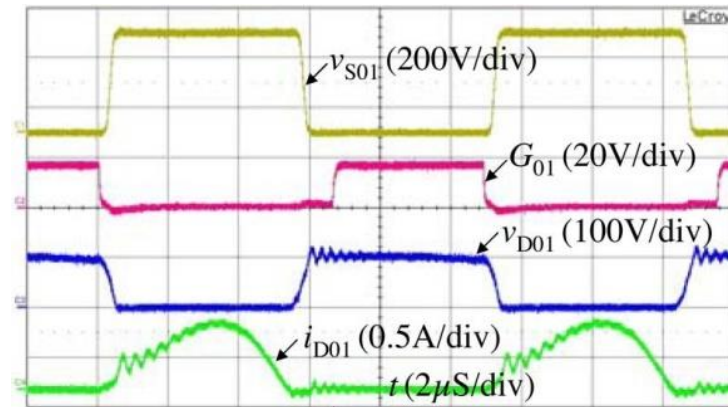


Fig. 7. displays the waveforms of MOSFET voltage $01vS01$ and its gate voltage $01vG01$, output diode voltage $01vD01$, and its current $01iD01$ in the LLC resonant converter.

S_{2n} and D_{2n} switching losses are both significantly decreased. The LED current amplitude I_n can be defined as the integral of the voltage delivered to the output inductor, which must be zero during every high switching cycle in the static state.

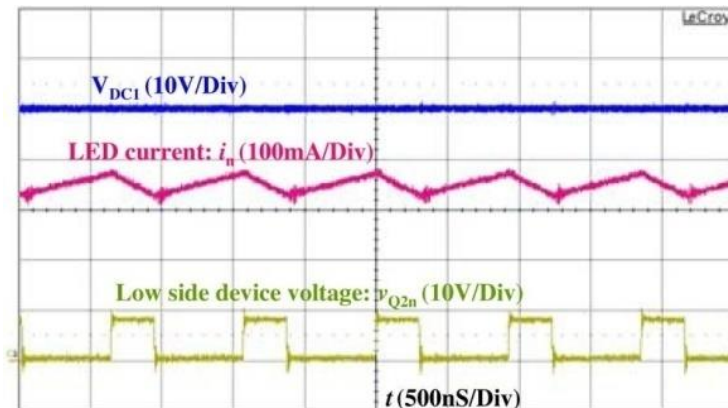


Fig. 8. shows the waveforms of input voltage $1V_{DC1}$, one string LED current, and low-side active device voltage.

LED; m is the number of series LEDs in each string; and D is the duty cycle of the bottom switch.

During the intervals shown in Fig. 3(a) and (b), the peak-to-peak current ripple can be expressed as follows:

$$I = V_{DC2} - m \cdot V_F + V_{DC1} - V_{DC2} \cdot D$$

$$\Delta I = m \cdot r_{LED} (V_{DC1} - m V_{LED}) D \cdot T$$

where $1V_{DC1}$ and $2V_{DC2}$ are the input voltages, and r_{LED} are the equivalent voltages and series resistances of each.

$$\Delta I_{pk} = (m V_{LED} - V_{DC2}) (1 - D) \cdot T$$

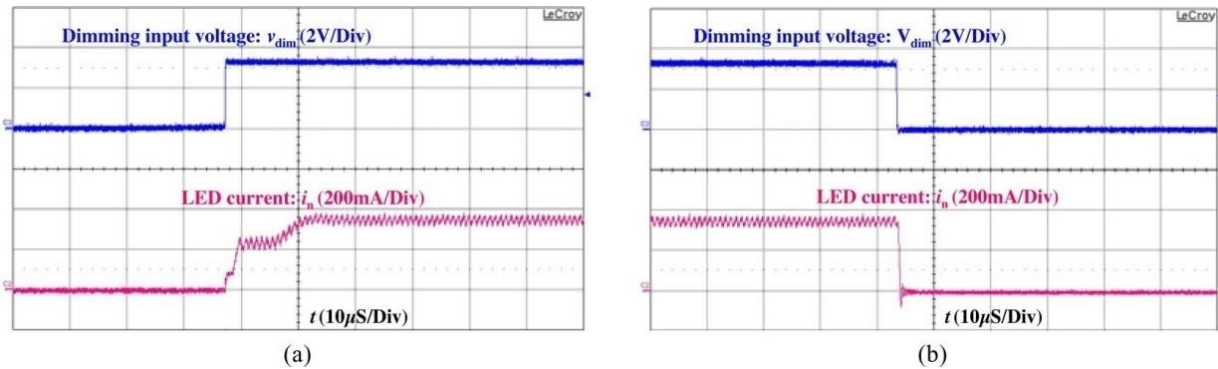


Fig. 9. presents the testing waveforms of LED current transition: (a) during the rising interval and (b) during the falling interval.

I. EXPERIMENTAL RESULTS

In order to verify the circuit validity and the improved performance of the proposed converter, a 50-W hardware prototype to drive three strings of 15 1.1-W high-brightness white LEDs was designed, manufactured, and tested. The power circuit and characteristics of the prototype aimed at off-line LED lighting applications are shown in Fig. 6, which includes the LLC resonant converter and the proposed twin-bus converter.

The LLC resonant converter regulates VDC1 by variable frequency modulation between 63 and 95 kHz using the standard isolated voltage feedback control loop. The twin-bus converter prototype includes the following parameters: 50 and 45 V of the twin-bus voltage, three strings of LEDs composed of 15 pieces of 1.1-W LEDs in series for each string, 400-Hz dimming frequency of the high-side switch, 1.08-MHz switching frequency of the low-side switches, 33- μ H output inductance, and the 350-mA rated LED current of each string. Three LM3407 integrated chips holding the low-side 1-/40-V constant current regulators regulators in place. To sense the current of each string, two 1.13- resistors are used in parallel. The 0.1-/100-V MOSFET and 1-A/100-V Schottky diode are the dimmable active and passive switches. The high-side driver circuit for the dimmable N-channel MOSFET is developed utilising the LM5101 with supplemental power from the additional winding in the front-end transformer. If the P-channel MOSFET with level-shift circuit is used as the dimming switch, the auxiliary power and high-side driver circuit can be omitted.

In the LLC resonant converter, the test results of the MOSFET device voltage vS01 and its gate voltage vG01, the output diode voltage vD01 and its current iD01 are shown in Fig. 7. The fact that vS01 goes to zero before its gate switches on clearly demonstrates that the MOSFET achieves zero-voltage switching. It can also be shown that the output diode turns on or off under zero-current switching conditions without a significant voltage spike. The experimental verification for the input voltage VDC1, the LED current of one string, and the low-side active device voltage at 1.08-MHz, 350-mA output current operations is shown in Fig. 8.

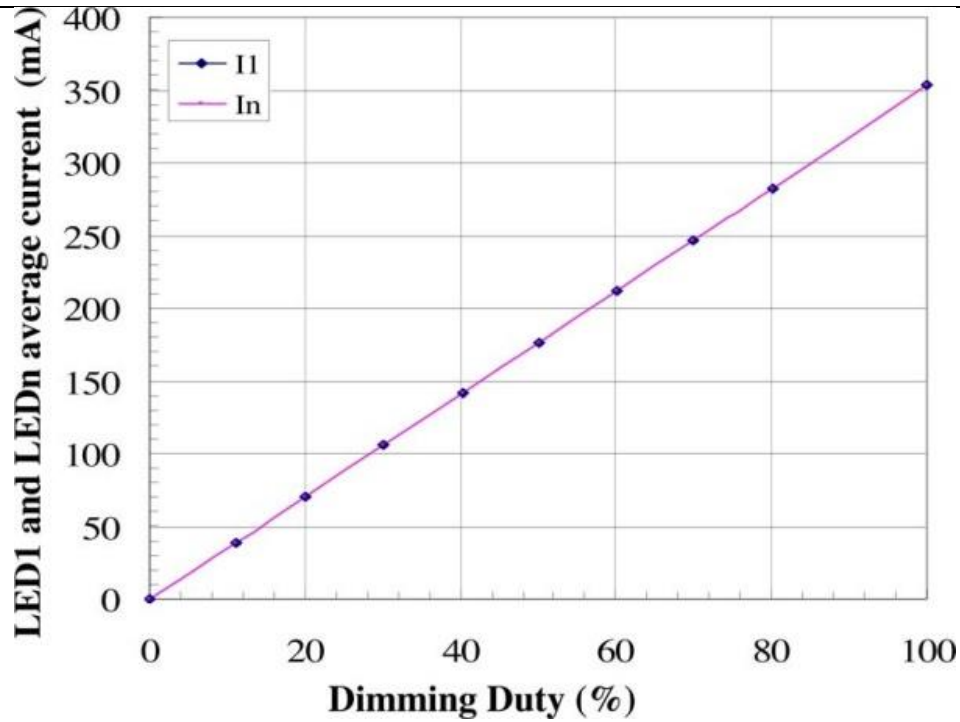


Fig. 10 illustrates the comparison of the average current of each LED string at different dimming duty cycles.

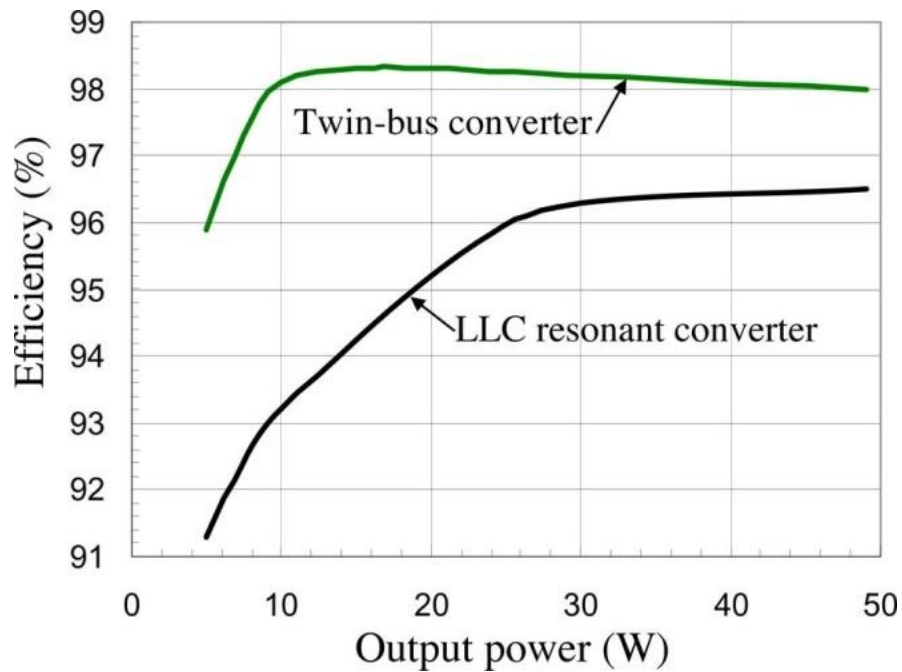


Fig. 11 presents the experimental results of efficiency as a function of the output current.

The LED current is effectively controlled, maintaining an average value of 352 mA with a peak-to-peak ripple of 17%. Additionally, the stress on the active switch is significantly low, ranging from 6 to 10 V, well below the 50 V input voltage.

Figure 9 illustrates the waveforms of the LED current transition during both rising and falling intervals. The slew rates of the LED current exceed 20 mA/s when using a 33 μ H output inductance, confirming the true zero-dimming capability of the proposed converter.

Figure 10 provides a comparison of the average current of each LED string at different dimming duties. It demonstrates strong linearity of each string's current over PWM dimming duty, with less than 0.2% current imbalance for each string.

In Figure 11, experimental efficiency is plotted as a function of output power for each string, with specified parameters including $V_{in} = 400$ V, $V_{DC1} = 50$ V, $V_{DC2} = 45$ V, $f_{S2n} = 1.08$ MHz, and 15 1.1-W LEDs in series. The twin-bus converter achieves peak efficiency of 98.3% and maintains efficiency above 98% for output power ranging from 10 to 50 W.

In conclusion, the novel converter with dual bus architecture presented in this study enables high-efficiency operation for dimmable LED lighting. It allows precise control of LED string currents from zero to the rated current level, with current-regulating switches operating at high switching frequencies and low voltage stresses. This design ensures high efficiency, compact size of output inductors, and fast LED current slew rates. Experimental results confirm the effectiveness of the proposed approach, achieving a maximum efficiency of 98.3% at a switching frequency of 1.08 MHz. Moreover, the utilization of tapped secondary-side windings enhances the efficiency of the front-end converter.

REFERENCES

- [1] Y. Hu and M. M. Jovanovic, "LED driver with self-adaptive drive voltage," *IEEE Trans. Power Electron.*, vol. 23, no. 6, pp. 3116–3125, Nov. 2008.
- [2] Z. Ye, F. Greenfeld, and Z. Liang, "Single-stage offline SEPIC converter with power factor correction to drive high brightness LEDs," in *Proc. IEEE Appl. Power Electron. Conf. Expo. (APEC'09)*, Feb. 15–19, pp. 546–553.
- [3] H.-J. Chiu, Y.-K. Lo, J.-T. Chen, S.-J. Cheng, C.-Y. Lin, and S.-C. Mou, "A high-efficiency dimmable LED driver for low-power lighting applications," *IEEE Trans. Ind. Electron.*, vol. 57, no. 2, pp. 735–743, Feb. 2010.
- [4] N. Prathyusha and D. S. Zinger, "An effective LED dimming approach," in *Proc. IEEE Ind. Appl. Soc. (IAS) Annu. Conf.*, Oct. 2004, pp. 1671–1676.
- [5] K. H. Loo, W.-K. Lun, S.-C. Tan, Y. M. Lai, and C. K. Tse, "On driving techniques for LEDs: Toward a generalized methodology," *IEEE Trans. Power Electron.*, vol. 24, no. 12, pp. 2967–2976, Dec. 2009.
- [6] X. R. Xu, "High dimming ratio LED driver with fast transient boost converter," in *Proc. IEEE Power Electron. Spec. Conf. (PESC)*, Jun. 2008, pp. 4192–4195.

-
- [7] D. Gacio, J. M. Alonso, A. J. Calleja, J. Garcia, and M. Rico, "A universal-input single-stage high power-factor power supply for HB-LEDs based on integrated buck-flyback converter," in Proc. IEEE Appl. Power Electron. Conf. (APEC), Feb. 2009, pp. 571–576.
- [8] K. N. Zhou, J. G. Zhang, Yuvarajan, and S. D. F. Weng, "Quasi-active power factor correction circuit for HB LED driver," IEEE Trans. Power Electron., vol. 23, no. 3, pp. 1410–1415, Mar. 2008.
- [9] X. H. Qu, S. C. Wong, C. K. Tse, and X. B. Ruan, "Isolated PFC pre-regulator for LED lamps," in Proc. Annu. Conf. Ind. Electron. (IECON), Nov. 2008, pp. 1980–1987.
- [10] S. Y. R. Hui and Y. X. Qin, "A general photo-electro-thermal theory for light emitting diode (LED) systems," IEEE Trans. Power Electron., vol. 24, no. 8, pp. 1967–1976, Aug. 2009.
- [11] J. Sebastian, P. J. Villegas, F. Nuno, O. Garcia, and J. Arau, "Improving dynamic response of power-factor preregulators by using two-input high-efficient postregulators," IEEE Trans. Power Electron., vol. 12, no. 6, pp. 1007–1016, Nov. 1997.
- [12] J. Sebastian, P. J. Villegas, F. Nuno, and M. M. Hernando, "High-efficiency and wide-bandwidth performance obtainable from a two-input buck converter," IEEE Trans. Power Electron., vol. 13, no. 4, pp. 706–717, Jul. 1998.
- [13] R. Redl, L. Balogh, and N. O. Sokal, "A new family of single-stage isolated power-factor correctors with fast regulation of the output voltage," in Proc. Power Electron. Spec. Conf. (PESC), Feb. 1994, pp. 1137–1144.
- [14] L. Gu, X. Ruan, M. Xu, and K. Yao, "Means of eliminating electrolytic capacitor in AC/DC power supplies for LED lightings," IEEE Trans. Power Electron., vol. 24, no. 5, pp. 1399–1408, May 2009.
- [15] B. Yang, F. C. Lee, A. J. Zhang, and G. Huang, "LLC resonant converter for front end DC/DC conversion," in Proc. Appl. Power Electron. Conf. (APEC), Feb. 2002, pp. 1108–1112.